

# Synthesis of Metal-Containing Poly(thiophene methines) via Solid- and Melt-State Polymerization and Their Related Applications as Highly Sensitive Ni<sup>2+</sup> Chemosensors

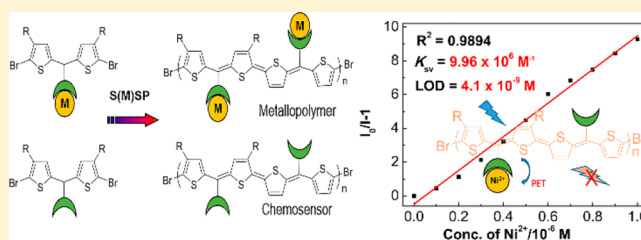
Qi Luo,<sup>†</sup> Kai Peng,<sup>†</sup> Jing Zhang,<sup>\*,†</sup> and Jiangbin Xia<sup>\*,†,‡</sup>

<sup>†</sup>College of Chemistry and Molecular Sciences, Wuhan University, Wuhan 430072, People's Republic of China

<sup>‡</sup>Engineering Research Center of Organosilicon Compounds & Materials, Ministry of Education, College of Chemistry and Molecular Sciences, Wuhan University, Wuhan 430072, People's Republic of China

## Supporting Information

**ABSTRACT:** Metal-containing polymers have attracted continuous interest, for they combine the features of a metal complex and a polymer. Here, a series of thiophene methine based phenanthroline ligands (L1–L4) and their metal (Zn(II) and Cd(II)) complexes were prepared as monomers. Accordingly, metal-containing poly(thiophene methines) were prepared from these metal complexes via solid- and melt-state polymerization (S(M)SP). The polymerization process was preliminarily investigated by a crystal structure study, NMR analysis, and absorbance spectra. Furthermore, the metal-free polymer (PL4) prepared directly from the ligand via MSP was tested as a metal ion chemosensor, which showed good selectivity and excellent sensitivity toward Ni<sup>2+</sup> with a detection limit of  $4.1 \times 10^{-9}$  M.



## INTRODUCTION

Metal-containing polymers (metallopolymers) have become a new branch of attractive materials due to their fascinating structures, unique optical-electronic, magnetic, physical, and chemical properties, and potential applications. For instance, metallopolymers can be designed as stimuli-responsive sensors,<sup>1</sup> which are responsive to physical stimuli (temperature,<sup>2,3</sup> electricity,<sup>4,5</sup> light,<sup>6</sup> and so on), chemical analytes (pH values,<sup>7</sup> gas molecules,<sup>8,9</sup> and ions,<sup>10–12</sup> etc.), or even biological signals.<sup>13,14</sup> For the practical and potential application of metallopolymers, a series of synthesis strategies have been developed. In general, the routes a metal is introduced into an organic polymer backbone can be classified into three categories.

(i) Introduction into the monomer before polymerization. In this way, the metal complex monomer should be chemically stable enough for the following polymerization process, or else demetalation would occur, as mentioned by other researchers.<sup>15</sup> Otherwise, the polymerization would not happen or invasive metal ions would be introduced because of their frequent involvement in the metal-catalyzed polymerization.

(ii) Introduction as a linkage while the metallopolymers grow, which is a self-assembled process.<sup>2,16</sup> The ligand-containing monomer used in this route should be carefully designed in accordance with the rules of coordination chemistry to obtain the desired structure.

(iii) Introduction after the ligand-containing polymer was synthesized, which has rarely been reported due to its intrinsic problems. On the one hand, it may face the same problem as

mentioned in the first category. In addition, even if the desired ligand-containing polymer is obtained successfully, the process of metal coordination would hardly proceed completely due to the great steric hindrance and cross-linking of the ligand-containing polymer. However, most of the conjugated polymers were obtained through metal-catalyzed polymerization methods, such as Pd-catalyzed Stille or Suzuki polycondensation. When these methods are applied to prepare metallopolymers, Pd(0) or Pd(II) may compete with metal ions especially under the harsh conditions of high temperature and long reaction time of 2–3 days. It is noted that few samples of metallocene-based conjugated polymers have been reported.<sup>17,18</sup> In addition, although other traditional methods of chemical oxidation and electropolymerization methods have already been applied, the big problem is that the generated strong acid (H<sup>+</sup>) would expel those metal ions significantly. For instance, 30–50% of Fe<sup>2+</sup> was lost in the porous Fe porphyrin polythiophene.<sup>19</sup>

In general, whatever the strategy used to prepare metallopolymers, the polymerization method using metal-containing catalysts should be avoided as much as possible. Thus, the big challenge facing us is to develop a universal approach to synthesize metal-containing conjugated polymers with accurate structure or ideal model, which is not only important for theoretical studies but also important to applied research. Recently, due to its special features of the absence of solvent,

Received: November 11, 2018



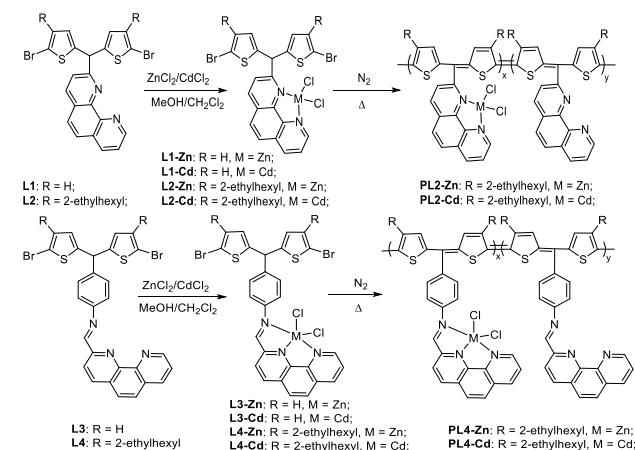
oxidant, or noble-metal catalyst, the promising method of solid-state polymerization (SSP) has attracted considerable attention since it was discovered in the early 1960s.<sup>20</sup> The application of SSP to thiophene derivatives was first proposed by Wudl in 2003<sup>21</sup> and was further studied by other researchers.<sup>22–28</sup> Briefly, polythiophene derivatives could be obtained by heating their monomers with the release of small molecules of halogens. Thus, such a bulk polymerization method would be a good choice for metallopolymer synthesis because there is no need to worry about the competition of different valence Pd catalysts with coordination moieties in polymer chains.

In view of the above research progress, we designed and synthesized two kinds of thienylene methine based ligands, 2-(bis(5-bromothiophen-2-yl)methyl)-1,10-phenanthroline and *N*-((1,10-phenanthroline-2-yl)methylene)-4-(bis(5-bromothiophen-2-yl)methyl)aniline, as well as the corresponding metal complex monomers. Then these complex monomers were subjected to bulk polymerization and their possible polymerization pathways were studied from the monomer crystal structures. The polymerization progress was preliminarily studied by <sup>1</sup>H NMR and UV–vis spectra. The obtained polymers were analyzed by FT-IR, gel permeation chromatography (GPC), and inductively coupled plasma atomic emission spectrometry (ICP). In addition, the polymer PL4 bearing these ligands was used as a chemosensor to detect metal ions and showed high sensitivity to Ni<sup>2+</sup> with a detection limit down to 4.1 × 10<sup>−9</sup> M, which is the most sensitive chemosensor to date.

## RESULTS AND DISCUSSION

**Synthesis and Characterizations.** The structures of bidentate ligands L1 and L2, tridentate ligands L3 and L4, and their metal complex monomers as well as their metallopolymer are shown in Scheme 1. The details of the

**Scheme 1. General Synthetic Routes to Metal Complexes L<sub>n</sub>-M and Metallopolymer PL<sub>n</sub>-M**



synthesis of ligands are available in Supporting Information. The monomers L1-Zn, L1-Cd, L3-Zn, and L3-Cd were designed as models to acquire the structure information on the complexes and to investigate the possible polymerization pathways. The 2-ethylhexyl group was introduced in the thiophene ring to improve the solubility of these polymers. PL2-Zn, PL2-Cd, PL4-Zn, and PL4-Cd were acquired by

heating their monomers under a nitrogen atmosphere for 12 h at 160–200 °C, respectively.

**Structure and Polymerization Analysis.** Single crystals of L1-Zn and L3-Zn were grown in a dichloromethane/diethyl ether mixture. These crystals were investigated by X-ray analysis to get the coordination information and thus to find the possible SSP/MSP polymerization pathways. As shown in Figure 1, both L1-Zn and L3-Zn adopt the ML coordinated

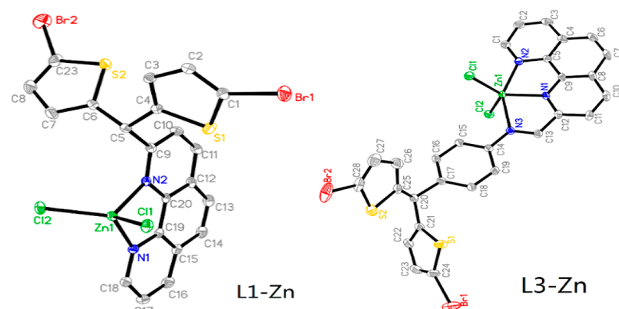


**Figure 1.** Crystal structures of L1-Zn and L3-Zn with thermal ellipsoids drawn at the 30% level. All hydrogen atoms and the solvents are omitted for clarity.

mode where each metal ion chelates with only a single ligand; thus, the tetracoordinated and pentacoordinated complex monomers are obtained, respectively. This coordination mode ensures that each monomer has only two active reaction sites for polymerization, and a merely one-dimensional polymer could be formed.

The crystal packing maps are shown in Figures 2 and 3. The Hal–Hal (halogen) and the corresponding C–C distances

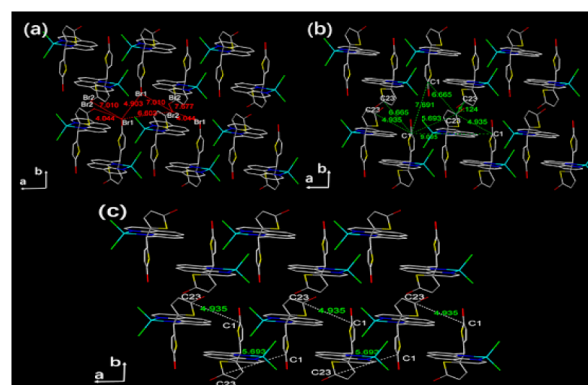


**Figure 2.** (a) Some Br–Br and (b) C–C distances in the crystal of L1-Zn. (c) The possible polymerization route of L1-Zn.

between adjacent monomers are marked as red and green dashed lines, respectively. The details are given in Table 1. In the case of L1-Zn, the shortest Hal–Hal distance is 4.044 Å along the *a* axis with the shortest C1–C13 distance of 4.935 Å. Although the Br1–Br1 distance along the *b* axis is the second shortest Hal–Hal distance (4.903 Å), the ultralong distance of C1–C1 (7.691 Å) makes the polymerization along the *b* axis impossible. The third shortest Hal–Hal distance is 6.602 Å with a C1–C23 distance of 5.693 Å, which is in a rational range for polymerization. Taking these different C–C and Hal–Hal distances into consideration, the most possible polymerization pathway of L1-Zn is along the *a* axis with the ...C1–C23–C1–C23... sequence (Figure 2c).

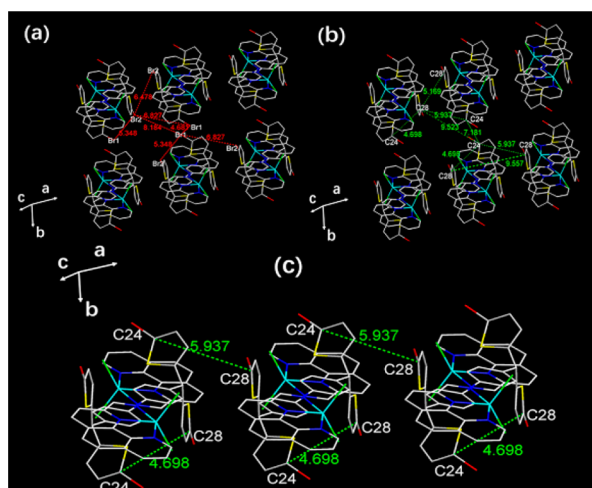


**Figure 3.** (a) Some Br–Br and (b) C–C distances in the crystal of L3-Zn. (c) The possible polymerization route of L3-Zn.

**Table 1.** Hal–Hal (Br–Br) and C–C Distances (Å) of Crystals L1-Zn and L3-Zn

molecules params	L1-Zn	L3-Zn
shortest Hal–Hal distance	4.044	4.681
second shortest Hal–Hal distance	4.903	5.348
third shortest Hal–Hal distance	6.602 <sup>a</sup>	6.478
fourth shortest Hal–Hal distance	7.010	6.827 <sup>a</sup>
C–C shortest contact distance	4.935	4.698
C–C second shortest contact distance	5.124	5.169
C–C third shortest contact distance	5.693	5.937
longer than $2r_w^b$ (%)	78	84

<sup>a</sup>Effective Hal–Hal distance. <sup>b</sup> $2r_w$ : double the van der Waals radius of bromine (3.7 Å).

In L3-Zn, the Br1–Br1 distance along the *b* axis is the shortest Hal–Hal distance (4.681 Å); however, the corresponding ultralong C24–C24 distance (7.181 Å) makes polymerization along the *b* axis impossible. The second shortest Hal–Hal distance of 5.348 Å with the shortest C–C distance of 4.698 Å makes C24–C28 the most possible unit in the polymers. The third shortest Hal–Hal distance is 6.478 Å with the second shortest C–C distance of 5.168 Å (C28–C28); however, only one C28–C28 bond could be formed in each polymer chain, as the C24–C24 distance is too long to form a C28–C24–C28–C28 chain. The most rational polymerization pathway of L3-Zn is along the *a* axis with the ...C24–C28–C24–C28... sequence (Figure 3c). In comparison to the metal-free ligand and other thiophene methine compounds reported by our group,<sup>29</sup> these metal-containing monomers have a higher onset temperature for polymerization, which may be ascribed to the longer Hal–Hal distances and stronger intermolecular interaction of metal complexes.

In order to investigate the structural variation during polymerization, L2-Zn and L4-Cd were chosen to heat at their onset temperatures (180 and 185 °C, respectively), and their <sup>1</sup>H NMR spectra in CDCl<sub>3</sub> were recorded each 2 h over a period of 12 h. As shown in Figure 4, the spectra of the L2-Zn mixture (L2-Zn-M) and L4-Cd mixture (L4-Cd-M) after heating for 0, 6, 8, 10, and 12 h are integrated, respectively. The poorer solubility and the unresolved NMR signals of aromatic H after a longer heating time are ascribed to the formation of polymers. Due to the limited solubility of the

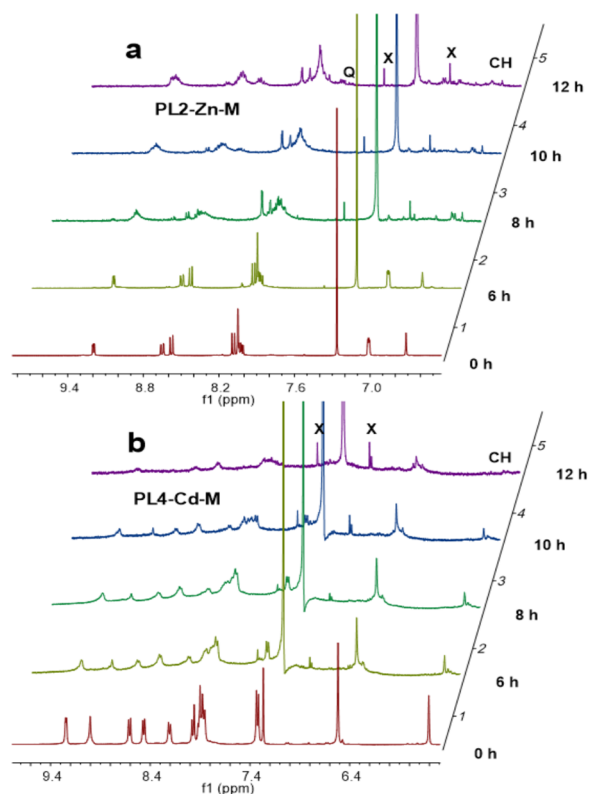


**Figure 4.** <sup>1</sup>H NMR spectra of L2-Zn-M (a) and L4-Cd-M (b) recorded after heating for 0, 6, 8, 10, and 12 h.

polymers, the dissolved fractions in CDCl<sub>3</sub> were subjected to NMR analysis to acquire their structural information. In the spectra of L2-Zn-M, the apparent reduction of signal intensity of the CH at 6.71 ppm and the observation of the quinonoid signals at 7.7–7.9 ppm (marked as Q in Figure 4a),<sup>30</sup> indicate the formation of a quinonoid structure in this metallopolymer. However, a series of weak peaks appearing around 6.71 ppm may account for the normal thiophene methine units where the CH units still remain. Similar changes are found in L4-Cd-M, except the quinonoid signals at 7.7–7.9 ppm are not obvious enough to be detected by <sup>1</sup>H NMR, revealing fewer quinonoid segments in L4-Cd-M. The sharp peaks X in the spectra are ascribed to an impurity of the deuterium reagent.

The absorption spectra of the heating mixtures were recorded to investigate the polymerization procedures. As shown in Figure 5a (L2-Zn-M), the most noteworthy change is the absorbance around 400 nm increasing with longer heating time: i.e., the absorbance value after heating for 12 h (value of 0.21) is about 20 times stronger than that of the starting monomer (value of 0.01). The absorption in the range of 320–

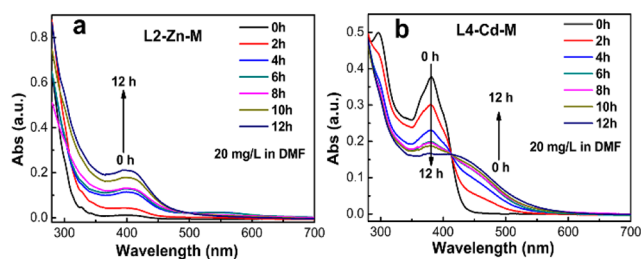


**Figure 5.** Optical spectra of L2-Zn-M (a) and L4-Cd-M (b) recorded after heating for 0–12 h in DMF.

450 nm is mainly assigned to the  $\pi$ - $\pi^*$  absorption bands of the aromatic heterocycle of the polymer repeat units. The stronger absorption may be due to the easier electron excitation process in the polymers. Moreover, the tail peaks appearing in the range of 450 nm to nearly 600 nm are assigned to the  $\pi$ - $\pi^*$  band gap transition of the polymers.<sup>31</sup> In Figure 5b (L4-Cd-M), the band around 380 nm is assigned to the  $\pi$ - $\pi^*$  band gap transition of the metal complex monomer. With an increase in heating time, the absorbance around 380 nm decreases and the absorption edge bathochromically shifts to about 600 nm. The absorption band that changes from a sharp peak (monomer) to an extended platform (polymer) may be ascribed to the lower band gap of the generated polymer. In view of the absorption spectra, the L4-Cd-M (12 h) shows an absorption band broader than that of L2-Zn-M (12 h). In comparison to L2, a phenyl group between CH and the coordinating group was introduced in L4 to weaken the steric hindrance, thus improving the conjugation degree of the polymer backbone of L4-Cd-M (12 h). All polymers show blue-shifted spectra in comparison to those of our previously reported polymers with similar skeletons,<sup>29</sup> which could be ascribed to the N-heterocycle in the monomer. The same phenomenon was also observed in the reported polymer containing the pyridyl<sup>32</sup> and our tentative SSP of 2-(bis(5-bromothiophen-2-yl)methyl)pyridine.

The preparation details and physical properties of the final polymers are given in Table 2. The molecular weights ( $M_n$ ) of

**Table 2. Preparation Details of Metallopolymers and Their Physical Properties**

	monomer			
	L2-Zn	L2-Cd	L4-Zn	L4-Cd
melting point, °C	162	166	172	175
reaction conditions	195 °C, 12 h	160 °C, 12 h	200 °C, 12 h	195 °C, 12 h
yield, %	78	80	85	83
$M_n$ of polymer, kDa	11.4	5.8	10.0	9.3
PDI	1.17	1.12	1.17	1.13
$T_{\text{onset}}$ , °C	180	146	188	185
DP	16	7	12	11
FTIR ( $\nu_{\text{C}=\text{C}}$ , $\text{cm}^{-1}$ )	1678	1676	1675	1672
FTIR ( $\nu_{\text{N}-\text{M}}$ , $\text{cm}^{-1}$ )	428	422	427	420
calcd metal content, %	8.7	14.2	7.6	12.5
tested metal content, %	3.4	4.3	4.0	5.1
metal remaining, %	39.1	30.2	52.6	40.8

the prepared polymers are in the range of 5.8–11.4 kDa, corresponding to a polymerization degree (DP) of 7–16. The structure information on those polymers was confirmed by FTIR. As shown in Figure 6, the absorption bands in the region of 2800–3000  $\text{cm}^{-1}$  are due to the C–H stretching vibration of the alkyl chain and aromatic rings. The C=C stretching vibrations of the thiophene and phenanthroline rings appear in the region of 1450–1620  $\text{cm}^{-1}$ . In comparison with the ligands L2 and L4, the newly weak absorption bands around 420  $\text{cm}^{-1}$  (marked as star) in their metal complex monomers are assigned to the metal–nitrogen bonds M–N (M = Zn, Cd), which could be observed in other reported similar metal complexes.<sup>33</sup> The M–N absorption signals are

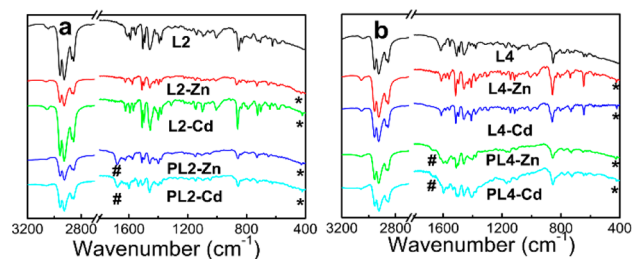


**Figure 6.** (a) FTIR absorption spectra of L2, L2-Zn, L2-Cd, PL2-Zn (195 °C) and PL2-Cd (160 °C) and (b) L4, L4-Zn, L4-Cd, PL4-Zn (200 °C) and PL4-Cd (195 °C).

still observed in their polymers, indicating the existence of chelating structures in these polymers. The metal ions were also detected by an ICP test (Table 2). The metal ions are partially lost from these polymers, which may be caused by the halogen or hydrogen halide generated during polymerization. Further reaction of metallopolymers PL4-Zn and PL4-Cd with the corresponding metal chloride could increase the metal remaining to some extent (Table S1). On the one hand, the halogen or hydrogen halide may expel the metal ions from the ligands. In addition, the perpendicular chelating group (C–(R)H) may be lost from the polymer at high temperature in the presence of halogen or hydrogen halide. There is another new absorption band around 1670  $\text{cm}^{-1}$  (marked as #) in the metallopolymers. This band is the characteristic absorption peak of the quinonoid bithienylene ring, which is in accordance with the NMR analysis (Figure 4).

Polymers containing coordination fragments are commonly employed as molecular hosts to chelate with transition-metal cations, and thereby some responses would appear from this variation. During this process, the conjugated polymer chains possess a magnified effect<sup>34</sup> toward the metal cation detection and inherently increase the detection sensitivity. Therefore, the polymer PL4, prepared from L4 by MSP at 130 °C, was used as a chemical sensor for detecting metal cations. The characterization of PL4, indicating that PL4 consists of a quinoid structure and aromatic structure in the ratio of 0.62/0.38, is available in the Supporting Information. Interestingly, as shown in Figure 7a, the monomer L4 shows very weak emission while PL4 shows strong emission and has a broad excitation wavelength from 275 to 425 nm, which may be ascribed to the extended conjugation of polymers. However, both of the metallopolymers PL4-Zn and PL4-Cd appear to be weakly emitting, indicating that the coordinated cations lead to

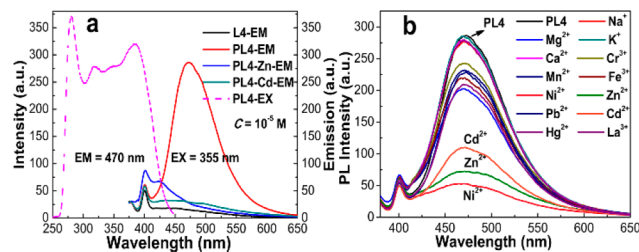


**Figure 7.** (a) Photoluminescence spectra of L4, PL4, PL4-Zn, and PL4-Cd (excitation: 355 nm) and excitation spectra of PL4 (emission: 470 nm). Concentration of monomer or polymer:  $10^{-5}$  M in DMF. (b) Photoluminescence spectra of PL4 in the presence of various metal ions (excitation: 355 nm). Concentration of polymer:  $10^{-5}$  M in DMF. Concentration of metal ions:  $5 \times 10^{-7}$  M in DMF.

fluorescence quenching of the polymers. Figure 7b shows the influence of various metal ions ( $\text{Na}^+$ ,  $\text{Mg}^{2+}$ ,  $\text{K}^+$ ,  $\text{Ca}^{2+}$ ,  $\text{Cr}^{3+}$ ,  $\text{Mn}^{2+}$ ,  $\text{Fe}^{3+}$ ,  $\text{Ni}^{2+}$ ,  $\text{Zn}^{2+}$ ,  $\text{Pb}^{2+}$ ,  $\text{Cd}^{2+}$ ,  $\text{Hg}^{2+}$ , and  $\text{La}^{3+}$ ) on the photoluminescence (PL) spectra of PL4 in DMF solution. Adding  $\text{Ni}^{2+}$ ,  $\text{Zn}^{2+}$ , and  $\text{Cd}^{2+}$  to the solution results in a significant decrease in PL intensity, indicating that these metal ions lead to efficient fluorescence quenching of PL4 and that PL4 shows good selectivity to these three cations. The PL intensity of PL4 shows no obvious change on addition of  $\text{Na}^+$ ,  $\text{K}^+$ ,  $\text{Ca}^{2+}$ , and  $\text{La}^{3+}$ , and the other cations also show a moderate fluorescence quenching effect on PL4.

Generally, the complexation of metal ions does not induce any shift of the emission peak. These results suggest that the fluorescence quenching behavior might be ascribed to the strong cation binding to the phenanthroline chelating groups, leading to the photoexcited energy transfer (PET) of the polymer chain.<sup>35,36</sup> It seems that both the diameters and charge densities of the metal ions that mainly determine the coordination strength can be regarded as substantial influences on the decreased fluorescence emission. The cations of  $\text{Na}^+$ ,  $\text{K}^+$ ,  $\text{Ca}^{2+}$ , and  $\text{La}^{3+}$  (larger than 2 Å) with a large diameter are adverse to chelating with the ligands, while  $\text{Ni}^{2+}$  (1.38 Å) and  $\text{Zn}^{2+}$  (1.48 Å) are in the proper diameter range and charge density to chelate with the polymers. In addition, the  $\text{Ni}^{2+}$  has an empty d orbital to accept the electron pair from the phenanthroline N, which not only strengthens the chelating binding but also facilitates the PET progress, thus leading to strong fluorescence quenching.

As shown in Figure 8a, the PL intensity decreases with an increase in concentration of the  $\text{Ni}^{2+}$  ion from 0 to  $10^{-6}$  M. It

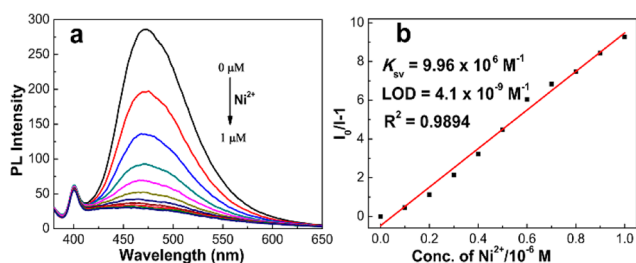


**Figure 8.** (a) Photoluminescence spectra (excitation: 355 nm) of PL4 in the presence of various concentrations of  $\text{Ni}^{2+}$  ion (0, 0.1, 0.2, 0.3, 0.4, 0.5, 0.6, 0.7, 0.8, 0.9, 1.0  $\mu\text{M}$ ). Concentration of polymer:  $10^{-5}$  M in DMF. (b) Stern–Volmer plot of PL quenching with various concentrations of  $\text{Ni}^{2+}$  ion.

is noted that more than 90% of the fluorescence was quenched while only 10% ( $10^{-6}$  M) of the ion relative to the ligand unit in polymer ( $10^{-5}$  M) was added, which could be explained by the amplification effect of the polymer. The quenching is approximately linear in this concentration range of  $\text{Ni}^{2+}$  (Figure 8b), while the Stern–Volmer constant ( $K_{\text{sv}}$ ) of PL4 toward  $\text{Ni}^{2+}$  is  $9.96 \times 10^6 \text{ M}^{-1}$ . Accordingly, the detection limit (LOD) is measured to be  $4.1 \times 10^{-9}$  M using the equation  $3\sigma/K_{\text{sv}}$ .<sup>37</sup> Table 3 summarizes some other reported sensitive  $\text{Ni}^{2+}$  chemosensors; our chemosensor has the highest  $K_{\text{sv}}$  value and the lowest LOD value toward  $\text{Ni}^{2+}$ . The ultrahigh sensitivity toward  $\text{Ni}^{2+}$  of this polymer could be ascribed to the strong coordination ability, good ligand–metal ion matching properties of the tridentate phenanthroline-based ligand, and the magnification effect of the conjugated polymer structure.

**Table 3.** Comparison of the Proposed Sensor with the Previously Reported  $\text{Ni}^{2+}$  Sensors

sensor for $\text{Ni}^{2+}$	$K_{\text{sv}}, \text{M}^{-1}$	detection limit, M	ref
2-amino-1-cyclopentene-1-dithiocarboxylic acid/acetyl cellulose membrane		$5.2 \times 10^{-7}$	38
2,5-thiophenylbis(5-tert-butyl-1,3-benzoxazole)/PVC membrane	$2.2 \times 10^5$	$8.0 \times 10^{-9}$	39
naphthalene-based chemosensor	$2.00 \times 10^4$	$8.0 \times 10^{-6}$	40
2-(1H-benzo[d]imidazol-2-yl)-N-phenylhydrazine carbothioamide	$7.08 \times 10^5$	$7.9 \times 10^{-8}$	41
imidazole derivative	$3.60 \times 10^4$	$2.8 \times 10^{-6}$	42
pyrenetetrasulfonic acid	$1.02 \times 10^5$	$6.4 \times 10^{-7}$	43
quinoline-based chemosensor		$3.7 \times 10^{-7}$	44
quinoline-based chemosensor	$5.03 \times 10^4$	$5.5 \times 10^{-7}$	45
pyrene-based chemosensor		$2.5 \times 10^{-7}$	46
naphthalene-based chemosensor		$1.9 \times 10^{-6}$	37
phenanthroline-based poly(thiophene methine) chemosensor	$9.96 \times 10^6$	$4.1 \times 10^{-9}$	this work

## CONCLUSION

Herein, two kinds of thiophene methine based phenanthroline ligands and their corresponding metal ( $\text{Zn}(\text{II})$  or  $\text{Cd}(\text{II})$ ) complexes were synthesized. The metallopolymers were prepared via SSP/MSP, and single crystals of L1-Zn and L3-Zn were used as models to analyze the possible polymerization pathways. NMR and UV–vis absorption were used to visualize the polymerization progress, and the obtained metallopolymers were characterized by FT-IR, GPC, and ICP analysis. In conclusion, a new strategy was presented for the synthesis of conjugated metallopolymers without use of any catalysts, despite metal ions being partially dissociated. In addition, polymer PL4 was employed as a metal cation sensor. This chemosensor shows good selectivity toward  $\text{Ni}^{2+}$ ,  $\text{Zn}^{2+}$ , and  $\text{Cd}^{2+}$  and shows excellent sensitivity to  $\text{Ni}^{2+}$  with a detection limit (LOD) of  $4.1 \times 10^{-9}$  M, which is the most sensitive chemosensor toward  $\text{Ni}^{2+}$  to date. In order to synthesize defect-free metallopolymers, further work with a carefully designed monomer structure is in progress.

## ASSOCIATED CONTENT

### Supporting Information

The Supporting Information is available free of charge on the ACS Publications website at DOI: 10.1021/acs.organomet.8b00830.

Synthesis and characterization details, NMR, and X-ray experimental details (PDF)

### Accession Codes

CCDC 1868215–1868216 contain the supplementary crystallographic data for this paper. These data can be obtained free of charge via [www.ccdc.cam.ac.uk/data\\_request/cif](http://www.ccdc.cam.ac.uk/data_request/cif), or by emailing [data\\_request@ccdc.cam.ac.uk](mailto:data_request@ccdc.cam.ac.uk), or by contacting The Cambridge Crystallographic Data Centre, 12 Union Road, Cambridge CB2 1EZ, UK; fax: +44 1223 336033.

## AUTHOR INFORMATION

### Corresponding Authors

\*E-mail for J.Z.: [jzhang03@whu.edu.cn](mailto:jzhang03@whu.edu.cn).

\*E-mail for J.X.: [jbxia@whu.edu.cn](mailto:jbxia@whu.edu.cn).

### ORCID

Jing Zhang: 0000-0003-4754-1659

Jiangbin Xia: 0000-0001-6238-4992

## Notes

The authors declare no competing financial interest.

## ACKNOWLEDGMENTS

We thank the Natural Science Foundation of China (21371138, 21875173), the Fundamental Research Funds for the Central Universities (2042015kf0180) of China, and the Large-scale Instrument And Equipment Sharing Foundation of Wuhan University for support. We thank Guang-Xiong Duan for help with the single-crystal X-ray diffraction measurements.

## REFERENCES

- (1) Zhang, K. Y.; Liu, S.; Zhao, Q.; Huang, W. Stimuli-Responsive Metallopolymers. *Coord. Chem. Rev.* **2016**, *319*, 180–195.
- (2) de Hatten, X.; Bell, N.; Yufa, N.; Christmann, G.; Nitschke, J. R. A Dynamic Covalent, Luminescent Metallopolymer that Undergoes Sol-to-Gel Transition on Temperature Rise. *J. Am. Chem. Soc.* **2011**, *133*, 3158–3164.
- (3) Miyata, K.; Konno, Y.; Nakanishi, T.; Kobayashi, A.; Kato, M.; Fushimi, K.; Hasegawa, Y. Chameleon Luminophore for Sensing Temperatures: Control of Metal-to-Metal and Energy Back Transfer in Lanthanide Coordination Polymers. *Angew. Chem., Int. Ed.* **2013**, *52*, 6413–6416.
- (4) Zeng, Q.; McNally, A.; Keyes, T. E.; Forster, R. J. Three Colour Electrochromic Metallopolymer Based on A Ruthenium Phenolate Complex Bound to Poly(4-vinyl)pyridine. *Electrochem. Commun.* **2008**, *10*, 466–470.
- (5) Matsui, J.; Kikuchi, R.; Miyashita, T. A Trilayer Film Approach to Multicolor Electrochromism. *J. Am. Chem. Soc.* **2014**, *136*, 842–845.
- (6) Borré, E.; Stumbé, J.-F.; Bellemin-Lapponnaz, S.; Mauro, M. Light-Powered Self-Healable Metallo-supramolecular Soft Actuators. *Angew. Chem., Int. Ed.* **2016**, *55*, 1313–1317.
- (7) Robinson, K. L.; Lawrence, N. S. Redox-sensitive Copolymer: A Single-Component pH Sensor. *Anal. Chem.* **2006**, *78*, 2450–2455.
- (8) Smith, R. C.; Tennyson, A. G.; Won, A. C.; Lippard, S. Conjugated Metallopolymers for Fluorescent Turn-on Detection of Nitric Oxide. *Inorg. Chem.* **2006**, *45*, 9367–9373.
- (9) Feng, X.; Sui, X.; Hempenius, M. A.; Vancso, G. J. Electrografting of Stimuli-responsive, Redox Active Organometallic Polymers to Gold from Ionic Liquids. *J. Am. Chem. Soc.* **2014**, *136*, 7865–7868.
- (10) Fan, L.-J.; Zhang, Y.; Jones, W. E. Design and Synthesis of Fluorescence “Turn-on” Chemosensors Based on Photoinduced Electron Transfer in Conjugated Polymers. *Macromolecules* **2005**, *38*, 2844–2849.
- (11) Shi, H.-F.; Liu, S.-J.; Sun, H.-B.; Xu, W.-J.; An, Z.-F.; Chen, J.; Sun, S.; Lu, X.-M.; Zhao, Q.; Huang, W. Simple Conjugated Polymers with On-chain Phosphorescent Iridium(III) Complexes: toward Ratiometric Chemodosimeters for Detecting Trace Amounts of Mercury(II). *Chem. - Eur. J.* **2010**, *16*, 12158–12167.
- (12) Fegley, M. E. A.; Sandgren, T.; Duffy-Matzner, J. L.; Chen, A.; Jones, W. E., Jr. Detection and Differentiation of Ferrous and Ferric Ions Using Fluorescent Metallopolymer and Oligomer Chemosensors. *J. Polym. Sci., Part A: Polym. Chem.* **2015**, *53*, 951–954.
- (13) Shi, H.; Ma, X.; Zhao, Q.; Liu, B.; Qu, Q.; An, Z.; Zhao, Y.; Huang, W. Ultrasmall Phosphorescent Polymer Dots for Ratiometric Oxygen Sensing and Photodynamic Cancer Therapy. *Adv. Funct. Mater.* **2014**, *24*, 4823–4830.
- (14) Zheng, X.; Wang, X.; Mao, H.; Wu, W.; Liu, B.; Jiang, X. Hypoxia-Specific Ultrasensitive Detection of Tumours and Cancer Cells in Vivo. *Nat. Commun.* **2015**, *6*, 5834.
- (15) Mak, C. S. K.; Cheung, W. K.; Leung, Q. Y.; Chan, W. K. Conjugated Copolymers Containing Low Bandgap Rhenium(I) Complexes. *Macromol. Rapid Commun.* **2010**, *31*, 875–882.
- (16) Asil, D.; Foster, J. A.; Patra, A.; Hatten, X. D.; Barrio, J. D.; Scherman, O. A.; Nitschke, J. R.; Friend, R. H. Temperature- and Voltage-induced Ligand Rearrangement of a Dynamic Electroluminescent Metallopolymer. *Angew. Chem., Int. Ed.* **2014**, *53*, 8388–8391.
- (17) Yamamoto, T.; Morikita, T.; Maruyama, T.; Kubota, K.; Katada, M. Poly(aryleneethynylene) Type Polymers Containing a Ferrocene Unit in the  $\pi$ -conjugated Main Chain. Preparation, Optical Properties, Redox Behavior, and Mössbauer Spectroscopic Analysis. *Macromolecules* **1997**, *30*, 5390–5396.
- (18) Abd-El-Aziz, A. S.; Todd, E. K.; Ma, G. Z. Design of Polyethers, Thioethers, and Amines with Pendent Iron Moieties. *J. Polym. Sci., Part A: Polym. Chem.* **2001**, *39*, 1216–1231.
- (19) Xia, J.; Yuan, S.; Wang, Z.; Kirklin, S.; Dorney, B.; Liu, D.-J.; Yu, L. Nanoporous Polyporphyrin as Adsorbent for Hydrogen Storage. *Macromolecules* **2010**, *43*, 3325–3330.
- (20) Magat, M. Polymerization in the Solid State. *Polymer* **1962**, *3*, 449–469.
- (21) Meng, H.; Peregichka, D. F.; Wudl, F. Facile Solid-state Synthesis of Highly Conducting Poly(ethylenedioxythiophene). *Angew. Chem., Int. Ed.* **2003**, *42*, 658–661.
- (22) Spencer, H. J.; Berridge, R.; Crouch, D. J.; Wright, S. P.; Giles, M.; McCulloch, I.; Coles, S. J.; Hursthouse, M. B.; Skabara, P. J. Further Evidence for Spontaneous Solid-State Polymerisation Reactions in 2,5-dibromothiophene Derivatives. *J. Mater. Chem.* **2003**, *13*, 2075–2077.
- (23) Patra, A.; Wijsboom, Y. H.; Zade, S. S.; Li, M.; Sheynin, Y.; Leitus, G.; Bendikov, M. Poly(3,4-ethylenedioxythiophene). *J. Am. Chem. Soc.* **2008**, *130*, 6734–6736.
- (24) Lepeltier, M.; Hiltz, J.; Lockwood, T.; Bélanger-Gariépy, F.; Peregichka, D. F. Towards Crystal Engineering of Solid-state Polymerization in Dibromothiophenes. *J. Mater. Chem.* **2009**, *19*, 5167–5174.
- (25) Tusy, C.; Huang, L.; Peng, K.; Xia, J. Parallel Design Strategy and Rational Study of Crystal Engineering of Novel 3,4-Ethylenedioxythiophene Derivatives for Solid State Polymerization. *RSC Adv.* **2014**, *4*, 29032–29041.
- (26) Huang, L.; Peng, K.; Pei, T.; Xia, J. Influence of Benzene Ring Number Attached on Non-conjugated 3,4-ethylenedioxythiophene Derivatives for Solid-state Polymerization. *RSC Adv.* **2015**, *5*, 70417–70423.
- (27) Peng, K.; Pei, T.; Li, Z.; Huang, L.; Xia, J. Investigation of the Substitution Effect on Poly(bis-3,4-ethylenedioxythiophene Methine)s Through Solid State Polymerization. *RSC Adv.* **2015**, *5*, 103841–103851.
- (28) Tusy, C.; Peng, K.; Huang, L.; Xia, J. Effect of Flexible Linker Length in 3,4-ethylenedioxythiophene Derivatives for Solid State Polymerization. *RSC Adv.* **2015**, *5*, 16292–16301.
- (29) Peng, K.; Pei, T.; Huang, N.; Yuan, L. J.; Liu, X. H.; Xia, J. Functionalization of Poly(bis-thiophene methine)s via Facile C–C Bulk Polymerization and Their Application as Chemosensors for Acid Detection. *J. Polym. Sci., Part A: Polym. Chem.* **2018**, *56*, 1676–1683.
- (30) Chen, W.-C.; Jenekhe, S. A. Small-bandgap Conducting Polymers Based on Conjugated Poly(heteroarylene methines). 2. Synthesis, Structure, and Properties. *Macromolecules* **1995**, *28*, 465–480.
- (31) Yang, M.; Zhang, Q.; Wu, P.; Ye, H.; Liu, X. Influence of the Introduction of Phenylene Units into the Polymer Backbone on Bandgap of Conjugated Poly(heteroarylene methines). *Polymer* **2005**, *46*, 6266–6273.
- (32) Jiang, K.; Cheng, X.; Cai, X.; Yanagida, S.; Xia, J. Exploring Novel Poly(thiophene-3-yl-amine) Through Facile Self Acid Assisted-polycondensation. *J. Polym. Sci., Part A: Polym. Chem.* **2017**, *55*, 4003–4012.
- (33) Anaconda, J. R.; Marquez, V. E.; Jimenez, Y. Synthesis and Characterization of Manganese(II), Nickel(II), Copper(II) and Zinc(II) Schiff-base Complexes Derived from 1,10-phenanthroline-2,9-dicarboxaldehyde and 2-mercaptoethylamine. *J. Coord. Chem.* **2009**, *62*, 1172–1179.

(34) Samori, P.; Biscarini, F. Nanomaterials Properties Tuned by Their Environment: Integrating Supramolecular Concepts into Sensing Devices. *Chem. Soc. Rev.* **2018**, *47*, 4675–4676.

(35) Dobrawa, R.; Lysetska, M.; Ballester, P.; Grüne, M.; Würthner, F. Fluorescent Supramolecular Polymers: Metal Directed Self-Assembly of Perylene Bisimide Building Blocks. *Macromolecules* **2005**, *38*, 1315–1325.

(36) Yang, P.-C.; Wu, H.; Lee, C.-L.; Chen, W.-C.; He, H.-J.; Chen, M.-T. Triphenylamine-Based Linear Conjugated Polyfluorenes with Various Pendant Groups: Synthesis, Characterization, and Ion Responsive Properties. *Polymer* **2013**, *54*, 1080–1090.

(37) Pannipara, M.; Al-Sehemi, A. G.; Irfan, A.; Assiri, M.; Kalam, A.; Al-Ammari, Y. S. AIE Active Multianalyte Fluorescent Probe for the Detection of  $\text{Cu}^{2+}$ ,  $\text{Ni}^{2+}$  and  $\text{Hg}^{2+}$  Ions. *Spectrochim. Acta, Part A* **2018**, *201*, 54–60.

(38) Ensafi, A. A.; Bakhshi, M. New Stable Optical Film Sensor Based on Immobilization of 2-amino-1-cyclopentene-1-dithiocarboxylic Acid on Acetyl Cellulose Membrane for Ni(II) Determination. *Sens. Actuators, B* **2003**, *96*, 435–440.

(39) Shamsipur, M.; Poursaberi, T.; Karami, A. R.; Hosseini, M.; Momeni, A.; Alizadeh, N.; Yousefi, M.; Ganjali, M. R. Development of a New Fluorimetric Bulk Optode Membrane Based on 2,5-thiophenylbis(5-tert-butyl-1,3-benzoxazole) for Nickel(II) Ions. *Anal. Chim. Acta* **2004**, *501*, 55–60.

(40) Banerjee, A.; Sahana, A.; Guha, S.; Lohar, S.; Hauli, I.; Mukhopadhyay, S. K.; Sanmartín Matalobos, J.; Das, D. Nickel(II)-induced Excimer Formation of a Naphthalene-based Fluorescent Probe for Living Cell Imaging. *Inorg. Chem.* **2012**, *51*, 5699–5704.

(41) Ganjali, M. R.; Hosseini, M.; Motalebi, M.; Sedaghat, M.; Mizani, F.; Faridbod, F.; Norouzi, P. Selective Recognition of  $\text{Ni}^{2+}$  Ion Based on Fluorescence Enhancement Chemosensor. *Spectrochim. Acta, Part A* **2015**, *140*, 283–287.

(42) Annaraj, B.; Mitu, L.; Neelakantan, M. A. Synthesis and Crystal Structure of Imidazole Containing Amide as a Turn On Fluorescent Probe for Nickel Ion in Aqueous Media. An Experimental and Theoretical Investigation. *J. Mol. Struct.* **2016**, *1104*, 1–6.

(43) Rambabu, D.; Pradeep, C. P.; Dhir, A. Nickel–sodium Pyrene Tetrasulfonic Acid Based Co-ordination Polymer as Fluorescent Template for Recognition of Azo Dyes. *Sens. Actuators, B* **2016**, *225*, 586–592.

(44) Senthil Murugan, A.; Vidhyalakshmi, N.; Ramesh, U.; Annaraj, J. A Schiff's Base Receptor for Red Fluorescence Live Cell Imaging of  $\text{Zn}^{2+}$  Ions in Zebrafish Embryos and Naked Eye Detection of  $\text{Ni}^{2+}$  Ions for Bio-analytical Applications. *J. Mater. Chem. B* **2017**, *5*, 3195–3200.

(45) Subashini, G.; Shankar, R.; Arasakumar, T.; Mohan, P. S. Quinoline Appended Pyrazoline Based  $\text{Ni}^{2+}$  Sensor and Its Application Towards Live Cell Imaging and Environmental Monitoring. *Sens. Actuators, B* **2017**, *243*, 549–556.

(46) Khan, R. I.; Ramu, A.; Pitchumani, K. Design and One-pot Synthesis of A Novel Pyrene Based Fluorescent Sensor for Selective “Turn on”, Naked Eye Detection of  $\text{Ni}^{2+}$  Ions, and Live Cell Imaging. *Sens. Actuators, B* **2018**, *266*, 429–437.